are bothered by the idea that ions with molecular weights of tens to hundreds of thousands and a single charge could desorb from a droplet surface. Moreover, we are bothered by some other features of the experiments and their interpretation. Along with the authors we find it difficult to understand why the repeller voltage at which ion transmission begins to decrease should decrease as the concentration of solute macromolecules decrease. This behavior can only mean that the ion mass is decreasing and that, therefore, at the higher solute concentrations the ions must contain more than one macromolecule. The assumption that we find most difficult to accept is that the final macroion velocity equals the terminal carrier gas velocity. Molecules much smaller than those used by Dole and his colleagues show "slip" effects resulting in substantial velocity deficits. Miller and Andres have developed a "slip Knudsen number" parameter that successfully correlates the experimental results of Abuaf et al.[40,41] Even optimistic estimates of the value of this parameter for Dole's experiments indicate that the macroions must have a velocity much less than the velocity of gas. In view of these considerations, we are inclined to think that at least some of Dole's ions might weel have comprised aggregates of macromolecules carrying more than one charge. Even so, his conception of the electrospray-bath gas-free-jet combination remains a powerful and important contribution.

Acknowledgment. This research has been supported in part by the National Science Foundation (Grant EGN-7910843) and the U.S. Department of Energy (Grant ET-78-G-01-3246). M.Y. acknowledges the cooperation and support of the Institute of Space and Astronautical Science that made his participation possible. J.B.F. is grateful to the Max-Planck Institute for Stroemungsforschung and the Alexander von Humboldt Foundation for providing the opportunity to prepare the manuscript.

(40) N. Abuaf, J. R. Anderson, R. P. Andres, J. B. Fenn, and D. R. Miller, "Rarefied Gas Dynamics, 5th Symposium", C. L. Brundin, Ed., Vol. 2, Academic Press, New York, 1966, p 1317.
(41) D. R. Miller and R. P. Andres, "Rarefied Gas Dynamics, 6th Symposium", L. Trilling and H. Wachman, Ed., Vol. 2, Academic Press, New York, 1969, p 1385.
(42) C. R. Blakley, J. J. Carmody, and M. L. Vestal, *Anal. Chem.*, **52** 1636 (1980).
(43) E. O. Hardin and M. L. Vestal, *Anal. Chem.*, **53**, 1492 (1981).
(44) C. R. Blakley and M. L. Vestal, *Anal. Chem.*, **55**, 750 (1983).

Pulsed Free Jets: Novel Nonlinear Media for Generation of Vacuum Ultraviolet and Extreme Ultraviolet Radiation

Charles T. Rettner,† Ernesto E. Marinero,† Richard N. Zare,*

Department of Chemistry, Stanford University, Stanford, California 94305

and Andrew H. Kung

San Francisco Laser Center, Department of Chemistry, University of California, Berkeley, California 94720
(Received: July 5, 1983)

We describe the application of free jets for the frequency tripling of laser radiation. Using a supersonic expansion of Xe we obtain $\sim 5 \times 10^{11}$ photons/pulse at 118.2 nm for an input power of 18 MW at 354.7 nm, while for CO we obtain $\sim 1 \times 10^{12}$ photons/pulse at 98.5 nm for an input power of 2 MW at 295.6 nm. In the latter case the conversion efficiency is enhanced by a two-photon resonance via the CO $A^1\Pi$ state. A simple model is presented for third harmonic generation in a free jet, and the predictions of this model are tested against experiment.

Introduction

Modern lasers provide intense, tunable, and essentially monochromatic light from the near-infrared to the ultraviolet. These sources have been extensively applied to chemical studies, greatly extending our knowledge of molecular spectroscopy, photochemistry, and state-selective reaction dynamics. However, many important molecular species (e.g., H_2, H_2O, N_2, CO) have their lowest electronically excited states in the vacuum ultraviolet (VUV), below ~185 nm. In order to apply laser techniques to study the spectroscopy and photochemistry of such species, and to access the Rydberg states of most molecules, it is necessary to develop tunable laser sources for this region. Unfortunately, the range of lasers operating in the VUV is rather restricted. Laser action has been demonstrated for only a handful of species, most notably H_2, F_2, CO, and the excimers of Xe, Kr, and Ar.[1] Furthermore, these can only operate on discrete lines and are consequently of limited value. For broadly tunable sources, a better approach is to frequency upconvert a high-power dye laser.

Frequency mixing and harmonic generation are well established as means of wavelength extension for visible lasers.[2,3] Typically, noncentrosymmetric crystals are employed as the upconverting (nonlinear) medium. However, the crystals in current use are all optically opaque below about 195 nm and therefore cannot be used for VUV generation. Instead it is necessary to employ gaseous nonlinear media,[4-10] such as rare gases or metal vapors. Numerous schemes have been described for the generation of coherent light throughout the VUV and even below the lithium fluoride cutoff (104 nm), in the extreme vacuum ultraviolet (XUV).[11-17] Some

† Present address: IBM Research Laboratory, 5600 Cottle Road, San Jose, CA 95193.

(1) S. C. Wallace, *Adv. Chem. Phys.*, **47**, 153 (1981).
(2) P. A. Franken, A. E. Hill, C. W. Peters, and G. Weinreich, *Phys. Lett.*, **7**, 118 (1961).
(3) M. D. Levenson, "Introduction to Nonlinear Laser Spectroscopy", Academic Press, New York, 1982.
(4) J. F. Ward and G. H. C. New, *Phys. Rev.*, **185**, 57 (1969).
(5) A. H. Kung, J. F. Yound, G. C. Bjorklund, and S. E. Harris, *Phys. Rev. Lett.*, **29**, 985 (1972).
(6) R. B. Miles and S. E. Harris, *I.E.E.E. J. Quantum Electron.*, **QE-9**, 470 (1973).
(7) A. H. Kung, J. F. Young, and S. E. Harris, *Appl. Phys. Lett.*, **22**, 301 (1973); **28**, 239 (E) (1976).
(8) R. T. Hodgson, P. P. Sorokin, and J. J. Wynne, *Phys. Rev. Lett.*, **32**, 343 (1974).
(9) A. H. Kung, *Appl. Phys. Lett.*, **35**, 653 (1974).
(10) K. K. Innes, B. P. Stoicheff, and S. C. Wallace, *Appl. Phys. Lett.*, **29**, 715 (1976).
(11) R. Hilbig and R. Wallenstein, *Opt. Commun.*, **44**, 283 (1983).
(12) E. E. Marinero, C. T. Rettner, R. N. Zare, and A. H. Kung, *Chem. Phys. Lett.*, **95**, 486 (1983).

0022-3654/84/2088-4459$01.50/0

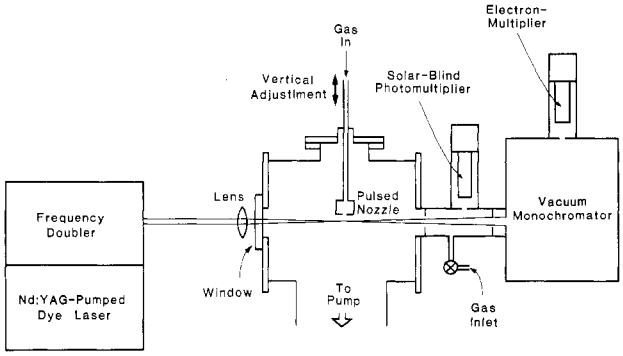

Figure 1. Experimental setup for frequency upconversion in a pulsed free jet.

have been developed sufficiently to permit application to fundamental problems in chemical physics. Notable examples include the detection of the Br product resulting from the reaction of H atoms with HBr[18] and the observation of nascent CO from the photolysis of formaldehyde.[19]

Most of the above laser schemes involve using a cell to contain the gaseous nonlinear medium. They are consequently limited in spectral coverage by the transmittance of available window materials. Differential pumping must be employed in cases where window materials are not available.[11,13,14] Recently we have demonstrated the versatility of pulsed free jets[20] in frequency upconversion. They provide a windowless environment which in addition minimizes the self-absorption of the generated radiation and the vacuum requirements for differential pumping.[12,21] In one study it was shown that 354.7-nm light can be efficiently tripled in a xenon jet to give $\sim 5 \times 10^{11}$ photons per shot at 118.2 nm,[21] while more recently we have demonstrated that a frequency-doubled dye laser can be frequency tripled in a jet to yield broadly tunable XUV radiation.[12] Here it was found that the addition of a T-shaped adapter enhanced the conversion efficiency. Using argon gas as the nonlinear medium we generated $\sim 10^{10}$ photons per shot over the range 97.3–102.3 nm. The resulting radiation was employed to detect molecular hydrogen via excitation of the Lyman and Werner band systems. We have also studied diatomic species to generate coherent VUV and XUV radiation[22] and developed a simple model that will predict the general behavior of the process for any single-component gaseous medium.[23] Bokor et al. have independently proposed the pulsed jet approach[16] and have utilized Xe and He jets to generate the third, fifth, and seventh harmonics of a picosecond excimer laser (KrF) to produce XUV radiation. The seventh harmonic at 35.5 nm represents the shortest wavelength coherent radiation reported in the literature to date.

In this paper, we present new data for frequency tripling in pulsed jets of Xe and CO and describe a simple model for the process of third harmonic generation close to the orifice of a free-jet expansion. For the CO study, we provide insights into the effect of rotational cooling by supersonic expansion on the XUV output. We also show that by exploiting a two-photon resonance via the CO $A^1\Pi$ state it is possible to achieve higher conversion efficiencies for the third harmonic generation process.

Experimental Section

Figure 1 displays a schematic drawing of the apparatus, as was described previously.[12,21] Only the essential features will be summarized here. The basic laser system consists of a Nd:YAG pumped frequency-doubled dye laser (Quanta-Ray, DCR-1A/PDL/WEX). The gaseous nonlinear medium is admitted through a 1.0-mm nozzle. This is sealed by a piezoelectrically driven plunger (Lasertechnics, LPV) and is opened synchronously with the firing of the laser so as to produce a pulsed free jet. Of considerable importance in predicting the properties of our free jet is the effective diameter of the nozzle employed. This diameter may be considerably smaller than the geometrical diameter if the plunger does not pull back far enough when in the open position. By comparing the gas load due to a pulsed argon jet with that produced by the expansion of a known quantity of air, we have arrived at an estimate for the effective nozzle diameter. Briefly, we find that a reservoir density of $N_0 = 6 \times 10^{19}$ atoms/cm^3 at 295 K leads to 2.4×10^{17} atoms/pulse over 276 μs (fwhm), giving an average flux of $F_p = 8.7 \times 10^{20}$ atoms/s. With the relationship[24]

$$F_p = N_0 V_0 A_{eff} \left(\frac{\gamma + 1}{2} \right)^{-[(\gamma+1)/(\gamma-1)]/2} \text{ atoms/s} \qquad (1)$$

which applies to an exit Mach number of unity, and

$$V_0 = (\gamma k T_0 / m)^{1/2} \text{ cm/s} \qquad (2)$$

where γ is the ratio of principal specific heats (5/3 for Ar and Xe and 7/5 for CO). For argon, $V_0 = 3.2 \times 10^4$ cm/s, giving $A_{eff} = 8.04 \times 10^{-4}$ cm^2, equivalent to a nozzle diameter of 0.32 mm. This is three times smaller than the geometric diameter, indicating that the failure of the plunger to retract completely is indeed limiting the flow. This effective area will be used in our calculations throughout this paper.

The valve assembly can be raised and lowered with respect to the top flange via a finely threaded drive which permits the nozzle to be positioned vertically to better than 0.3 mm. The laser is focused within the jet with a single 20-cm focal length fused silica lens held on an XYZ translation stage. Careful measurements of the frequency-doubled dye laser beam profile, using a knife edge held on a separate translation stage, revealed a confocal parameter, $b = 0.8$ cm. The confocal parameter is defined as twice the distance between the beam waist and that point where the beam area reaches twice its focal point value. For the 354.7-nm beam, a b value of 0.4 cm was obtained from a frequency tripling experiment using a cell of xenon, as will be described later.

Third harmonic VUV and XUV light are detected by an electron multiplier (EMI Model D233) mounted at the exit of a separately pumped 0.3-m vacuum monochromator (McPhereson Model 218). Gases (e.g., H_2) can be admitted to a short section between the monochromator and main chamber in order to perform absorption or fluorescence experiments. These experiments provide an estimate of the third harmonic intensity and line width. All gases are of research purity (>99.99%) and are used without further purification.

A liquid-nitrogen-trapped 6-in. diffusion pump (NRC, Model VHS-6) backed by a rotary pump (Sargent Welch, Model 1397) is used to maintain a background pressure in the main chamber of $\lesssim 10^{-4}$ torr during the experiments. A 2-in. diffusion pump (NRC Model 189) is used to supplement the evacuation of the monochromator.

Results

Xe. Figure 2 shows the dependence of the third harmonic signal at 118.2 nm on the incident energy of the 354.7-nm beam. The data points were taken by focusing the laser 1 mm downstream

(13) H. Egger, R. T. Hawkins, J. Bokor, H. Pummer, M. Rothschild, and C. K. Rhodes, *Opt. Lett.*, **5**, 282 (1980).
(14) H. Egger, T. Srinivasan, K. Boyer, H. Boyer, and C. K. Rhodes, "Laser Techniques for Extreme Ultraviolet Spectroscopy", American Institute of Physics Conference Proceedings No. 90, T. J. McIlrath and R. R. Freeman, Eds., American Institute of Physics, New York, 1982, p 445.
(15) J. Reintjes, *Opt. Lett.*, **4**, 242 (1979).
(16) J. Bokor, P. H. Bucksbaum, and R. R. Freeman, *Opt. Lett.*, **8**, 217 (1983).
(17) J. Reintjes, C.-Y. She, and R. C. Eckart, *I.E.E.E. J. Quantum Electron.*, **Q.E-14**, 581 (1978).
(18) J. W. Hepburn, D. Klimek, K. Liu, R. G. Macdonald, F. J. Northrup, and J. C. Polanyi, *J. Chem. Phys.*, **74**, 6226 (1981).
(19) P. Ho and A. V. Smith, *Chem. Phys. Lett.*, **90**, 407 (1982).
(20) W. R. Gentry and C. F. Giese, *J. Chem. Phys.*, **67**, 5389 (1977); *Phys. Rev. Lett.*, **39**, 1259 (1977); *Rev. Sci. Instrum.*, **49**, 595 (1978).
(21) A. H. Kung, *Opt. Lett.*, **8**, 24 (1983).
(22) A. H. Kung, unpublished results.
(23) C. T. Rettner, unpublished results.
(24) See, for example, J. B. Anderson in "Molecular Beams and Low Density Gas Dynamics", P. P. Wegener, Ed., Marcel Dekker, New York, 1976, p 1.

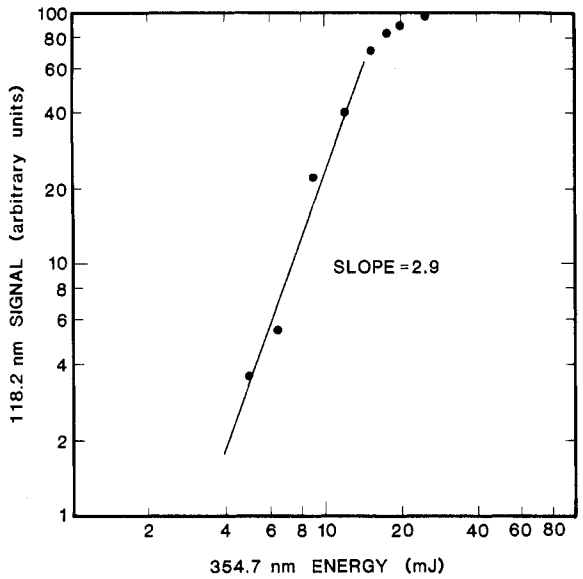

Figure 2. Third harmonic power as a function of the incident laser energy.

from the nozzle exit and using a xenon reservoir density of 4.2 × 10^{19} atoms/cm^3. The 118.2-nm signal varies linearly with incident energies below about 10 mJ, yielding a slope of d[log (signal)]/d[log (energy)] = 2.9 ± 0.1.

We are able to estimate the absolute number of VUV photons produced by each laser pulse by using an acetone-filled ionization cell as a proportional counter.[21] We find that for incident UV energies of 10 mJ (2 MW) we generate ~6 × 10^{10} photons at 118.2 nm in 2.9-ns pulses, giving a peak VUV power of ~30 W. These values can be used to place Figure 2 on an absolute scale. Using an input power of 18 MW yielded ~5 × 10^{11} photons per pulse, the maximum VUV signal obtained.

We have also examined the 118.2-nm signal dependence on the distance, X, from the nozzle exit to the laser beam axis. The crosses in Figure 3 show a typical result. This result was for a reservoir density of 3.8 × 10^{19} atoms/cm^3.

Finally, Figure 4 displays the dependence of the 118.2-nm signal on the relative delay between the laser firing and the nozzle triggering. This was obtained with a 200-μs, 100-V triggering pulse. The flat top indicates that the nozzle was operating in a pressure-limited flow regime.

CO. For CO, the doubled dye laser wavelength was chosen so as to excite two-photon transitions of the CO $A^1\Pi$–$X^1\Sigma^+$ system. Tuning the laser frequency across the (2,0) band, we observe dramatic enhancements in the third harmonic signal at the line position of individual rotational members of the O, P, Q, R, and S branches (ΔJ = −2, −1, 0, +1, and +2, respectively). The resulting spectra mirror the rotational populations of the ground $X^1\Sigma(v''=0)$ state and are thus very sensitive to the degree of rotational cooling produced by the expansion. Figure 5 displays the spectra obtained with the laser focused at a number of different distances from the nozzle. The values of X (defined as the distance from the nozzle to the laser beam axis) are indicated in each case. The rotational band assignments[25] are indicated at the top of the figure. By comparing the XUV signals recorded for CO with those measured previously for frequency tripling in argon,[12] at the same wavelength, we estimate the absolute maximum intensities of the generated radiation to be ~1 × 10^{12} photons/pulse for an incident power of ~2 MW (10 mJ).

It is clear from Figure 5 that the signal dependence on X varies considerably for the different rotational levels accessed. We have analyzed a series of carefully calibrated spectra to obtain the variation of third harmonic signals with X for the S(1), S(2), S(3), and S(4) lines (corresponding to J'' = 1–4). These data are displayed in Figure 6, where experimental points are indicated by crosses.

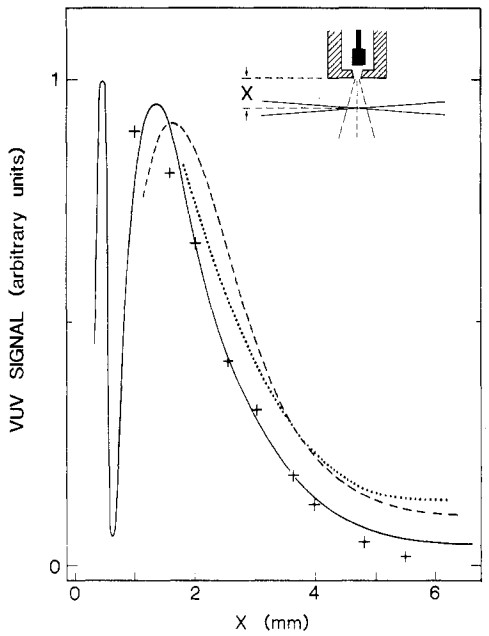

Figure 3. VUV intensity as a function of the distance between the nozzle and the laser beam axis for frequency tripling 354.7-nm radiation in Xe. The experimental points are indicated as crosses while curves are calculated (see Discussion). Here the reservoir density of Xe is N_0 = 3.8 × 10^{19} cm^{-3}.

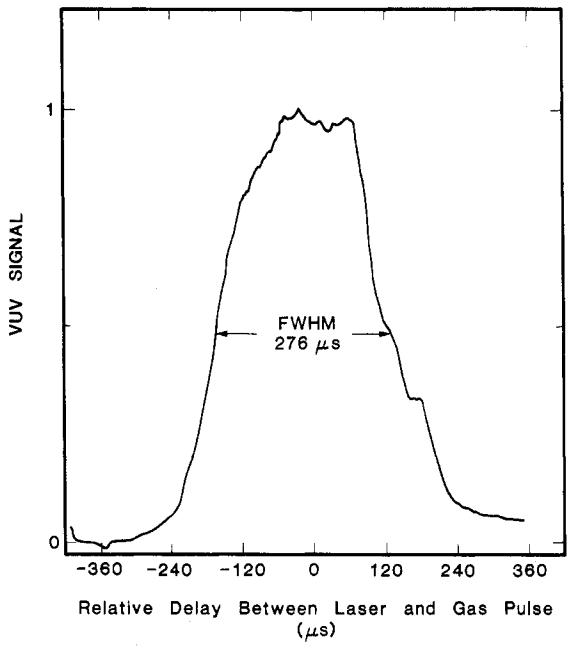

Figure 4. Dependence of third harmonic power on the delay between the nozzle and laser pulses.

Discussion

Frequency Tripling in Free Jets. We have demonstrated that a pulsed free jet can be employed as the nonlinear medium for efficient third harmonic generation. For a laser wavelength λ_1 of power P_1 incident on a gaseous medium of density N and third-order susceptibility $\chi_3(\lambda_3)$, the conversion efficiency is given (in SI units) by[4,6,26,27]

$$\frac{P_3}{P_1} = \frac{3\pi^2}{\epsilon_0{}^2 c^2 \lambda_1{}^4} N^2 [\chi_3(\lambda_3)]^2 P_1{}^2 |\Phi|^2 \qquad (3)$$

(25) J. D. Simmons, A. M. Bass, and S. G. Tilford, *Astrophys. J.*, **155**, 345 (1969).

(26) R. B. Miles, Ph.D. Thesis, Stanford University, 1972.

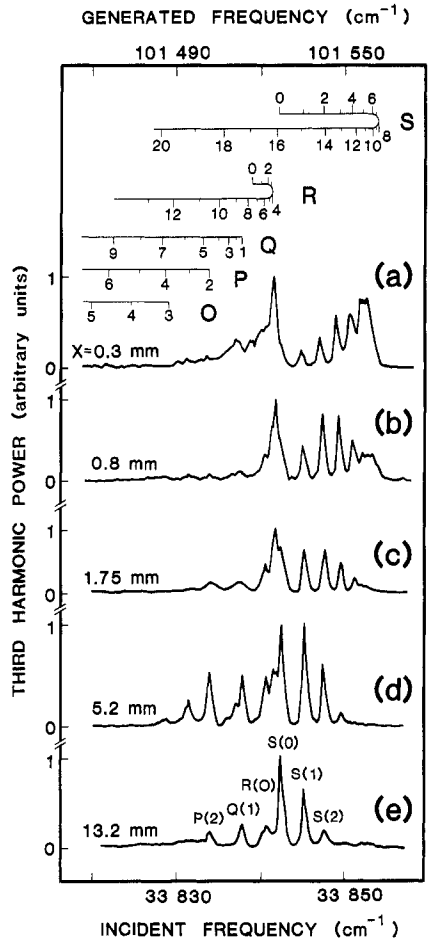

Figure 5. Two-photon-resonant frequency tripling in CO. The $A^1\Pi$–$X^1\Sigma^+$ (2,0) band is utilized to enhance the XUV signal. The distance between the nozzle exit and the laser beam axis is indicated on each trace and in all cases the reservoir density of CO is $N_0 = 9.14 \times 10^{19}$ cm^{-3}.

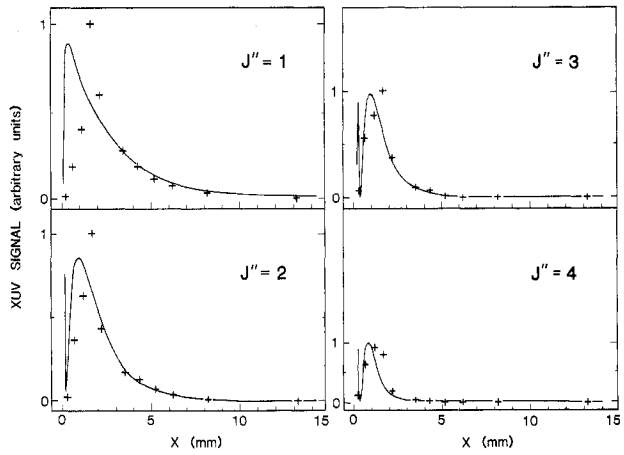

Figure 6. Variation of the third harmonic power with the distance between the nozzle and the laser beam axis for frequency tripling in CO. Experimental points are indicated by crosses while the solid curves were obtained from the model presented in the text (see Discussion). Results are shown for $J'' = 1$–4, which were obtained by tuning to the S(1) to S(4) transitions of the CO $A^1\Pi$–$X^1\Sigma^+$ (2,0) band for a CO reservoir density of $N_0 = 9.14 \times 10^{19}$ cm^{-3}.

where P_3 is the third harmonic power of wavelength λ_3 and $|\Phi|^2$ is a (dimensionless) geometric factor which accounts for the effects of focusing and dispersion. Here $\chi(\lambda_3)$ has units of m^5 V^{-2}. However, since susceptibilities are most commonly expressed in cgs electrostatic units (where $\chi(\lambda_3)$ has units of esu) a more convenient practical form of eq 3 is that given by Miles and Harris[6,26]

$$\frac{P_3}{P_1} = \frac{8.215 \times 10^{-2}}{\lambda_1^4} N^2 [\chi_3(\lambda_3)]^2 P_1^2 |\Phi|^2 \qquad (4)$$

which is arrived at by using $\chi(\lambda_3)_{SI} = (4\pi/9) \times 10^{-14} \chi(\lambda_3)_{esu}$.[27] Here, P is expressed in W, λ in cm, and N in particles cm^{-3}. For a Gaussian beam incident on a sample of length, L, which is short compared to the confocal parameter of the laser beam, b, $|\Phi|^2$ reduces to the plane-wave limit given by[6,26]

$$|\Phi|_{pw}^2 = \left[(2L/b) \frac{\sin(\Delta kL/2)}{(\Delta kL/2)} \right]^2 \qquad (5)$$

where Δk is the wavevector mismatch defined in terms of the refractive indices at the generated and incident wavelength as $\Delta k = k_3 - 3k_1 = 6\pi(n_3 - n_1)/\lambda_1$. Miles[26] has shown that this relationship holds well up to $b \geq 3L$. Since b values tend to be of the order of several millimeters, this relationship should certainly apply to the case of focusing a laser beam close to the orifice of a typical free jet.

An alternative arrangement, when window materials permit, is to focus within the body of a sample of length $L >> b$. Then $|\Phi|^2$ takes the tight focusing result of[6,26]

$$|\Phi|_{tf}^2 = [(\pi b \Delta k) \exp(b\Delta k/2)]^2 \quad \Delta k < 0 \qquad (6)$$

$$= 0 \quad \Delta k \geq 0$$

In this tight focusing case the conversion efficiency, which we define as $E_{tf} = P_3/P_1$, reaches a maximum for $b\Delta k = -4$. On the other hand, for a given gas, the conversion efficiency in the plane-wave limit, E_{pw}, reaches a maximum for $L\Delta k = n\pi$, where n is an odd integer. Realizing that Δk can be written as $N\Delta C$, where ΔC is the phase mismatch per atom,[29] we find that

$$E_{tf}(\max)/E_{pw}(\max) = 2.89 \quad \Delta k < 0 \qquad (7)$$

$$= 0 \quad \Delta k \geq 0$$

Hence we conclude that, by working close to the plane-wave limit, *third harmonic generation in a free jet can be almost as efficient as that for tight focusing, when Δk is negative, and is infinitely better for positive Δk.* In addition, E_{tf} may be lowered by self-absorption of the generated wave over the long pathlengths involved[26] and E_{pw} can potentially be greatly improved by optimizing Δk through phase matching by the addition and mixing of a second gas.[6,7,26,28-31] In the absence of a jet, similar conversion efficiencies can be achieved by focusing close to a window or pinhole.[11,13,14] However, these methods do not permit the same versatility of experimental design. Focusing at a window is limited by the damage threshold of the window material, while the pinhole approach puts constraints on the vacuum achievable in adjacent chambers.

As mentioned above, eq 5 holds for $b \gtrsim 3L$. In fact this relationship is still a reasonable approximation for $L \sim b$. For our experiments, this is equivalent to $L \sim 1$ cm, a length considerably greater than the width of our free jet close to the orifice. Thus we expect the observed conversion efficiency in a free jet to be given by

$$E_{fj} \cong \frac{1.314N^2}{\lambda_1^4 b^2 \Delta k^2} [\chi_3(\lambda_3)]^2 P_1^2 \sin^2(\Delta kL/2) \qquad (8)$$

(27) For details for units, see also D. C. Hanna, M. A. Yuratich, and D. Cotter, "Nonlinear Optics of Free Atoms and Molecules", Springer-Verlag, New York, 1979.

(28) G. C. Bjorklund, *I.E.E.E. J. Quantum Electron.*, **QE-11**, 287 (1975).
(29) R. Mahon, T. J. McIlrath, V. P. Myerscough, and D. W. Koopman, *I.E.E.E. J. Quantum Electron.*, **QE-15**, 444 (1979).
(30) R. Mahon and Y. Mui Yiu, *Opt. Lett.*, **5**, 279 (1980).
(31) H. Puell, H. Scheingraber, and C. R. Vidal, *Phys. Rev. A*, **22**, 1165 (1980).

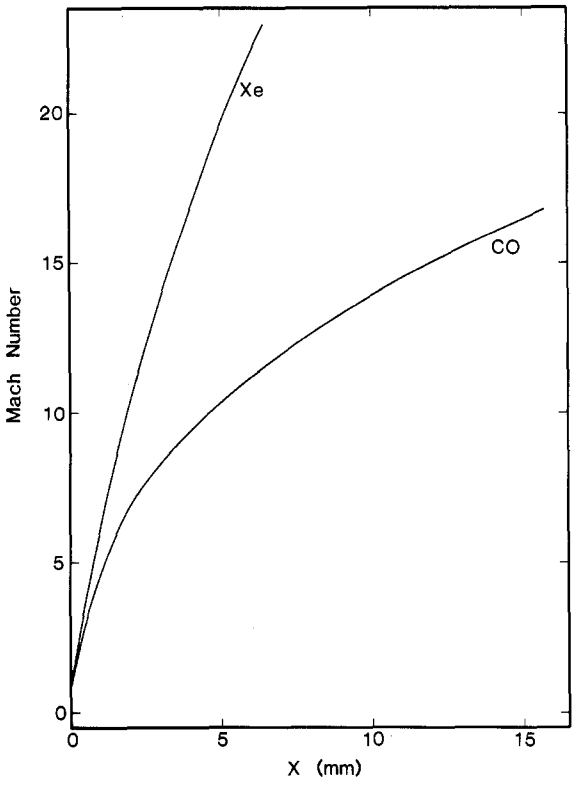

Figure 7. Calculated variation of Mach number with distance from the nozzle exit for Xe and CO based on eq 11 and 12 with a value of D = 0.32 mm.

Using $\Delta k = N\Delta C$ and $A_0 = \lambda_1 b/4$, where A_0 is the Gaussian area of the laser beam at its focal point, we obtain

$$E_{fj} \cong \frac{8.125 \times 10^{-2}}{\lambda_1^2 \Delta C^2}[\chi^3(\lambda_3)]^2\left[\frac{P_1}{A_0}\right]^2 \sin^2(\Delta kL/2) \quad (9)$$

Note that in this approximation E_{fj} retains a dependence on the jet density only through the $\sin^2(\Delta kL/2)$ term, which may actually equal unity at any point in the jet where $\Delta kL = \Delta CNL = n\pi$, as mentioned above.

To apply eq 9 to predict the third harmonic conversion efficiency for focusing onto a free jet, we need to obtain expressions for the jet density along the direction of propagation of the laser beam. We begin by assuming that the jet density perpendicular to the X direction has a rectangular profile. In this picture, the on-axis density, $N(X)$, extends out to some distance equal to $L(X)/2$ and then drops to zero. In reality the density profile will of course be more complex[32] and strictly this should be convoluted with the laser profile to obtain $|\Phi(X)|^2$. However, it seems unlikely that a closed form for this quantity could be obtained.

The jet density, $N(X)$, is related to the Mach number, M, in the beam by[24,32]

$$N(X) = \frac{N_0}{\left(1 + \frac{(\gamma - 1)}{2}M^2\right)^{1/(\gamma-1)}} \quad (10)$$

where M can be estimated according to the fitting formulas of Ashkenas and Sherman,[32] whereby for $\gamma = 5/3$

$$M(X) = 3.26(X/D - 0.075)^{2/3} - 0.61(X/D - 0.075)^{-2/3} \quad (11)$$

and for $\gamma = 7/5$

$$M(X) = 3.65(X/D - 0.4)^{2/5} - 0.82(X/D - 0.4)^{-2/5} \quad (12)$$

Here D is the effective diameter of the nozzle. The variation of M with X for Xe and CO predicted by these expressions is displayed in Figure 7.

(32) H. Ashkenas and F. S. Sherman, *Rarefied Gas Dyn.*, **3**, 84 (1966).

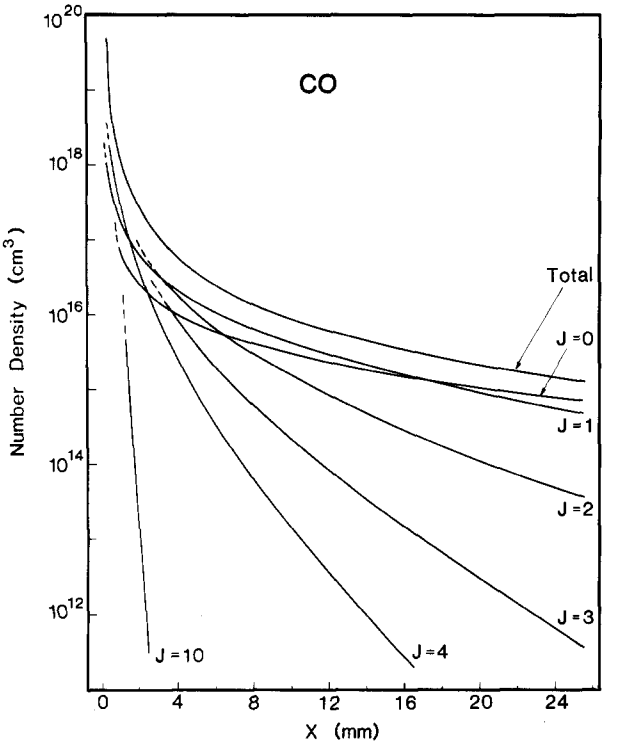

Figure 8. Calculated rotational population for CO as a function of distance from the nozzle. These results were obtained by using eq 10, 12, and 13 for $N_0 = 9.14 \times 10^{19}$ cm^{-3} and D = 0.32 mm.

In CO, $N(X)$ is dominated by the number density of the rotational state with quantum number J that is two-photon resonant with the incident radiation

$$N(X,J) = \frac{N(X)(2J + 1)\exp(-J(J + 1)B/kT(X))}{\sum_{J=0}^{\infty}(2J + 1)\exp(-J(J + 1)B/kT(X))} \quad (13)$$

where B = 1.93 cm^{-1} is the rotational constant of the CO $X^1\Sigma^+$ state, and $T(X)$ is the temperature in the jet, given by[24]

$$T(X) = \frac{T_0}{1 + \left(\frac{\gamma - 1}{2}\right)M^2} \quad (14)$$

Here we are assuming that there is a minimal rotational lag, i.e., the rotational temperature in the expansion is equal to the isentropic value. At large X/D values some degree of rotational "freezing" is likely to occur, but in the high density region of the jet of concern here, eq 14 is expected to be a good approximation.[33] Figure 8 displays the variation of $N(X,J)$ for CO(J'' = 1, 2, 3, and 4) as calculated from the above equations by using D = 0.32 cm and $N_0 = 9.14 \times 10^{19}$ cm^{-3}.

The path length through the jet at X, $L(X)$, may be estimated by considering the conservation of particle flux through all planes perpendicular to X. At all X this flux must be the same as that issuing from the nozzle, F_p, discussed in the Experimental Section. We take the flow velocity at X, $V(X)$, as[24]

$$V(X) = M(X)(\gamma kT(X)/m)^{1/2} \quad (15)$$

where T is given by eq 14 and $M(X)$ by eq 11 or 12. Thus the flux at X is given by

$$F(X) = N(X)V(X)\pi L(X)^2/4 = \frac{1}{4}N_0V_0\pi L(X)^2M(X)\left[1 + \frac{(\gamma - 1)}{2}M(X)^2\right]^{-[(\gamma+1)/(\gamma-1)]/2} \quad (16)$$

(33) J. J. Repetski and R. E. Mates, *Phys. Fluids*, **14**, 2605 (1971), and references contained therein.

setting $F(X) = F_p$ given by eq 1 we obtain

$$L(X) = \frac{D}{M(X)^{1/2}}\left[\frac{2 + (\gamma - 1)M(X)^2}{\gamma + 1}\right]^{[(\gamma+1)/(\gamma-1)]/4} \quad (17)$$

Thus for Xe, using $D = 0.32$ mm, we obtain for the path length (in mm)

$$L(X) = \frac{0.240}{M(X)^{1/2}}\left(1 + \frac{M(X)^2}{3}\right) \quad (18)$$

while for CO

$$L(X) = \frac{0.243}{M(X)^{1/2}}\left(1 + \frac{M(X)^2}{5}\right)^{3/2} \quad (19)$$

The variation of L with X for Xe and CO is shown in Figure 9. Here we see that, in both cases, L increases linearly with X after the first few millimeters. Extrapolating the linear portion of these curves back through $X = 0$ we find an intercept of $L \sim 0$, corresponding to a point close to the center of the nozzle. This is consistent with the finding that the flow streamlines in a jet at $X/D > 4$ radiate from a point on the jet axis close to the nozzle exit plane.[24,32]

To complete our model, we wish to introduce one additional factor to allow for the fact that the laser beam area is not fixed at the focal point value of A_0 but expands on either side of the focus. This effect can be accounted for by replacing $1/A_0^2$ by $\langle A(Z)^{-2}\rangle_L$, the average value of the inverse of the square of the beam area taken over $-L/2$ to $+L/2$. For a Gaussian laser beam, the area at a distance Z from the waist is given by[34]

$$A(Z) = A_0\left(1 + \frac{4Z^2}{b^2}\right) \quad (20)$$

Then

$$\langle A(Z)^{-2}\rangle_L = \frac{1}{A_0^2 L}\int_{-L/2}^{L/2}\frac{dZ}{(1 + 4Z^2/b^2)^2} = \frac{1}{2A_0^2}\left[\frac{1}{(1 + (L/b)^2)} + \left(\frac{b}{L}\right)\tan^{-1}\left(\frac{L}{b}\right)\right] \quad (21)$$

Combining eq 9 and 21 we get

$$E_{fj}(X) = \frac{4.06 \times 10^{-2}}{\lambda_1^2 \Delta C^2}[\chi_3(\lambda_3)]^2\left(\frac{P_1}{A_0}\right)^2 \times \sin^2(\Delta C\, N(X)\, L(X)/2)\left[\frac{1}{1 + (L(X)/b)^2} + \left(\frac{b}{L(X)}\right)\tan^{-1}\left(\frac{L(X)}{b}\right)\right] \quad (22)$$

Let us now consider the experimental results presented for Xe and CO.

Xe. The cubic dependence of P_3 and P_1 found for third harmonic generation in jets of xenon (Figure 2) is readily understood, noting that $P_3 = P_1 E_{fj}$. For $P_1 \gtrsim 2$ MW, an approximately linear increase of P_3 with P_1 was observed. This corresponds to a "saturation" intensity of $\sim 6 \times 10^{11}$ W/cm^2. Similar saturation effects have been reported previously for this same process.[35]

In ref 21 it was shown that an input power of $P_1 = 2$ MW at 354.7 nm focused onto a xenon jet at $X = 1$ mm gave a maximum VUV power of ~ 30 W, yielding $E_{fj}(\max) \simeq 1.5 \times 10^{-5}$. Now using $\chi_3(\lambda_3) = 5.6 \times 10^{-36}$ esu/atom[7] and $\Delta C = -5.99 \times 10^{-17}$ cm^2,[28] we can substitute into eq 22 to obtain a calculated value of $E_{fj}(\max)$. We arrived at a value of b by carrying out a separate experiment where the laser was focused into a long cell of Xe. The optimum pressure of 5.1 torr obtained in this case[21] gives Δk

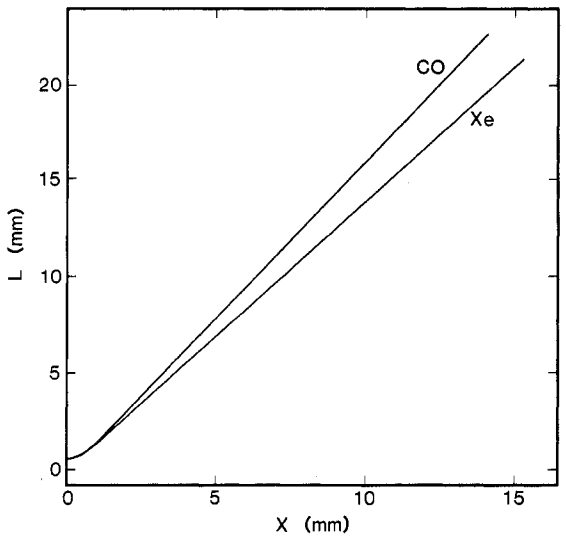

Figure 9. Variation of the calculated effective interaction length, L, with the distance between the nozzle and the laser beam axis based on eq 18 and 19 with $D = 0.32$ mm.

$= N\Delta C = -10.0$ cm^{-1}. Using $(\Delta kb)_{max} = -4$ for tight focusing,[6,28] we obtain $b = 0.4$ cm. Our model predicts $\sin^2(\Delta C\, N(X)\, L(X)/2) = 1$ at $X = 1.25$ mm at which point $L/b = 0.425$ and E_{fj} is predicted to be 1.6×10^{-5}. Thus, apart from misplacing the maximum by 0.25 mm, there is good agreement between the simple model and experiment. Clearly, for higher input powers, where saturation effects become large, eq 4 and 22 can no longer be considered valid.

Having set the reservoir density to produce an optimum conversion efficiency for $X = 1$ mm, we investigated the variation of E_{fj} with X out to $X \sim 6$ mm. This data were shown in Figure 3. We may now compare these results with the predictions of eq 22, based on the expressions given for $N(X)$ and $L(X)$ in eq 10, 11, and 18. We find an optimum fit for $N_0 = 3.05 \times 10^{19}$ atoms/cm^3 rather than the measured value of 3.8×10^{19} atoms/cm^3. This is shown as the solid curve in Figure 3. The dashed curve displays the fit obtained with $N_0 = 3.8 \times 10^{19}$ atoms/cm^2. Notice that the model predicts a rapid oscillation in the conversion efficiency for $X \lesssim 1$ mm. This is due to the $\sin^2(\Delta CNL/2)$ term in eq 8 and 22 and indicates that, for $X \lesssim 1$ mm, $\Delta CNL > \pi$. Finally, the dotted curve shows the effect of omitting the correction factor $\langle A^{-2}\rangle_L$. We see that eq 22 can indeed quantitatively predict the conversion efficiency for third harmonic generation in a free jet of xenon. If ΔC had been unknown, we note that using the measured value of N_0 would have yielded a value for ΔC of -4.8×10^{-17} cm^2. Comparing the fits with and without the $\langle A^{-2}\rangle_L$ correction factor we see that this factor accounts for most of the error involved in using eq 5 rather than the exact integral.

CO. It is clear from the spectra presented in Figure 5 that the third harmonic generation process in CO is greatly enhanced when the incident wavelength matches a two-photon transition to the CO $A^1\Pi$ state. This is in accord with the findings of Wallace and Innes who studied third harmonic generation in NO,[10,36] and Vallee, Wallace, and Lukasik[37] who examined 4-wave sum frequency mixing in CO. This enhancement arises predominantly through increases in the third-order nonlinear susceptibility, $|\chi_3(\lambda_3)|$, which may be written as[36]

$$|\chi_3(\lambda_3)| \propto \sum_{m,n}\{\langle X^1\Sigma^+(v'',J'')|\mu|n\rangle\langle n|\mu|A^1\Pi(v',J')\rangle \times \langle A^1\Pi(v',J')|\mu|m\rangle\langle m|\mu|X^1\Sigma^1(v'',J'')\rangle / [(E_n - 3\hbar\omega_1)(E_A(\Delta v,\Delta J) - 2\hbar\omega_1 - i\Gamma)(E_m - \hbar\omega_1)]| \quad (23)$$

where each index is summed over all electronic states of CO. Here E_n, E_A, and E_m are the energies of the nth, $A^1\Pi$, and mth states

(34) See, for example, J. T. Verdeyen, "Laser Electronics", Prentice-Hall, Englewood Cliffs, New Jersey, 1981, p 60.
(35) L. J. Zych and J. F. Young, *I.E.E.E. J. Quantum Electron.*, **QE-14**, 147 (1978).
(36) S. C. Wallace and K. K. Innes, *J. Chem. Phys.*, **72**, 4805 (1980).
(37) F. Vallee, S. C. Wallace, and J. Lukasik, *Opt. Commun.*, **42**, 148 (1982).

connected by electric dipole matrix elements, with the appropriate dipole operators, μ. The resonance behavior of $\chi_3(\lambda_3)$ in the region of transitions to the $A^1\Pi$ state is contained in the factor $(E_A - (\Delta v,\Delta J) - 2\hbar\omega_1 - i\Gamma)$, where $E_A(\Delta v,\Delta J)$ is the transition energy, $2\hbar\omega_1$ is the two-photon energy, and $i\Gamma$ is a line profile term which prevents singularities from arising. Thus when $2\hbar\omega_1 = E_A(\Delta v,\Delta J)$, this term equals $-i\Gamma$, which will be of the order of the laser bandwidth, ~ 1 cm^{-1}, for these studies. This will be many orders of magnitude smaller than when there is no resonant intermediate state, where $(E_A - 2\hbar\omega_1)$ can be in the range 10^3–10^5 cm^{-1}.

In their NO studies,[36] Wallace and Innes found that the third harmonic intensities varied as the square of the two-photon line strengths,[38,39] which is to be expected when a single state, the $C^2\Pi$ state in their case, acts as the m and n states in eq 20. For these CO studies, no such simple relationship is apparent. This may be due to competition between third harmonic generation and multiphoton ionization of CO. Such behavior has been observed previously for this molecule[40] in the case of three-photon-enhanced third harmonic generation via the same CO $^1\Pi(v'=2)$ state, using light around 443 nm. Alternatively, we may be seeing effects due to interference between different terms in the susceptibility, which can become important if either two different species are present or if two types of nonlinear processes are simultaneously selected.[41]

Notwithstanding the uncertainty in the relevant effective line strengths for the different rotational levels, it will be clear from the spectra presented that the jet becomes very rotationally cold as the expansion proceeds. For example, at $X = 3.5$ mm we estimate a rotational temperature of ~ 20 K, while for $X = 13.2$ mm it appears to be less than 5 K.

Let us examine the variation of third harmonic conversion efficiency with distance from the nozzle. These data were presented in figure 6. Using eq 10, 12, and 13 to predict $N(X,J)$ and eq 12 and 19 for $L(X)$, we have tested eq 22 against these experimental results, for $J'' = 1$–4. Since ΔC for CO is unknown for our wavelengths, this was necessarily an adjustable parameter. Rather than vary ΔC for each rotational state, a single best-fit value was sought. The solid curves presented in Figure 6 were obtained for $\Delta C = -9 \times 10^{-17}$ cm^2. The peak heights were scaled according to S(1):S(2):S(3):S(4) equals 1:0.8:0.6:0.4, compared to the two-photon line strengths of 1:0.78:0.67:0.62 and the square of these of 1:0.61:0.45:0.38.

It will be clear that the simple model can indeed predict the general growth and decay curves for this process, but that it fails to match the exact position of the peaks. In each case, we predict a peak at around 1 mm earlier than it actually occurs. Increasing ΔC to push this peak out to match the data results in a failure to fit the long-distance "tail", the theoretical curve staying high relative to the results.

There are of course many possible reasons for these discrepancies, such as the approximations used in the model and the ill-defined nature of the particular pulsed valve employed. From the point of view of the free-jet relationships used, it is certainly an approximation to assume a rectangular profile for the jet, particularly as it is known that the temperature profile varies considerably along this axis.[24] However, the succes with fitting the xenon data suggests that this can explain only part of the discrepancy. It may be that there is indeed a significant difference between the rotational temperature of CO and the isentropic value given by eq 14. In addition, as suggested above, there may be interference terms in $\chi_3(\lambda_3)$ and/or competition with multiphoton ionization. Further, resonances at the three-photon level could be present, which cause ΔC to vary across the spectrum. Considering the many uncertainties involved, further discussion must await the results of additional experimental data.

Finally, we emphasize that the simple model presented should only be considered valid for $X \lesssim b$, at which point the plane-wave relationship employed in its derivation becomes a progressively worse approximation. These limitations may be overcome by setting

$$|\Phi(L/b)|^2 = f(L/b)|\Phi|_{pw}^2 + [1 - f(L/b)]|\Phi_{tf}|^2 \quad (24)$$

i.e., taking a linear combination of the plane-wave and tight-focusing results. This approximation is suggested by the fact that the exact results for $|\Phi(L/b)|^2$ are found to vary smoothly between these two limiting relationships.[26,28] Thus the relationship given in eq 24 may have much practical value in estimating the mismatch factor $|\Phi|^2$.

Conclusion

We have shown that a free jet can be employed as a versatile nonlinear medium for the generation of third harmonic radiation. Quantitative relationships have been developed to predict conversion efficiencies, and these have been found to agree closely with data for Xe and CO. These relationships reflect a complex interplay between three factors at a given distance between orifice and the laser beam axis: (i) the beam density, (ii) the effective beam width, and, for the case of molecules, (iii) the rotational quantum state distribution in the beam. It is hoped that this work will be of use to others in planning experiments which exploit free jets as the nonlinear medium in the generation of VUV and XUV radiation.

Acknowledgment. This work was supported in part by the Office of Naval Research under N000014-78-C-0403 and the National Science Foundation under NSF CHE 81-08823 and NSF CHE 79-16250. R.N.Z. also gratefully acknowledges support through the Shell Distinguished Chairs program, funded by the Shell Companies Foundation, Inc.

Registry No. Xe, 7440-63-3; CO, 630-08-0.

(38) R. G. Bray and R. M. Hochstrasser, *J. Mol. Spectrosc.*, **31**, 412 (1976).
(39) J. B. Halpern, H. Zacharias, and R. Wallenstein, *J. Mol. Spectrosc.*, **79**, 1 (1980).
(40) J. H. Glownia and R. K. Sander, "Laser Techniques for Extreme Ultraviolet Spectroscopy", American Institute of Physics Conference Proceedings No. 90, T. J. McIlrath and R. R. Freeman, Eds., American Institute of Physics, New York, 1982, p 465.
(41) M. D. Levenson and N. Bloembergen, *J. Chem. Phys.*, **60**, 1323 (1974).